JOURNAL OF CATALYSIS 116, 71–81 (1989)

Preparation of Ternary Cu/Co/Al Catalysts by the Amorphous Citrate Process

I. Decomposition of Solid Amorphous Precursors

J. I. DI COSIMO AND C. R. APESTEGUÍA

Instituto de Investigaciones en Catálisis y Petroquímica, INCAPE, Santiago del Estero 2654, 3000 Santa Fe, Argentina

Received January 20, 1988; revised June 3, 1988

Cu–Co–Al amorphous precursors were prepared by means of the citric complexing method. The atomic ratios $R = (Cu + Co)/Al$ and $r = Cu/Co$ were varied between $12 \geq R \geq 1$ and $5 \geq r \geq 0.5$. The thermal decomposition of solid citrate precursors was carried out in air and nitrogen, and characterized by DTA, derivative thermogravimetry (DTG), and IR spectroscopy. Results showed that the main steps of the decomposition in air were (i) an exothermic transformation at 135–150°C which represented a mass loss of $\Delta W = 25$–35%, (ii) an intermediate decomposition at 220–240°C of $\Delta W = 10$–12%, and (iii) a highly exothermic decomposition at 280–300°C of $\Delta W = 20$–25%. IR spectra indicated that the low-temperature decomposition was caused by an exothermic reaction between ionic nitrates and free carboxyl groups. The high-temperature stage corresponded to the oxidation of the citric acid structure. When decomposition was performed in N_2, the DTG curves allowed us to distinguish between two main regions. Up to 280°C the DTG patterns were very similar to those observed for the decomposition in air. Above 280°C, the treatment in N_2 caused the breakup of the citrate chains through several consecutive transformations. In all the cases, the main characteristics of the decomposition peaks depended on the metallic composition. The decomposition of the precursors in air showed a high tendency to uncontrolled decomposition. On the other hand, after the N_2 treatment at 500°C a significant content of carbon remained on the samples. The advantage of performing a two-step decomposition procedure using first nitrogen up to 280°C and after that an air atmosphere to oxidize the organic part of precursors at relatively low temperature is particularly discussed in this paper.

INTRODUCTION

The use of methanol as a single gasoline blend component poses problems like phase separation when water is present and a significant increase in the Reid vapor pressure (RVP). These two critical problems can be overcome by incorporating a mixture of higher alcohols (normal and isopropanol, normal and isobutanol, and C_5 and C_6 alcohols) as cosolvent into the methanol–gasoline blend. The mixture of methanol with C_2–C_6 alcohols has been called methyl fuel (*1*), alkanol fuel (*2*) and MAS (*3*). Since, in the early seventies, Vulcan Inc. confirmed the possibility of producing from synthesis gas a C_1–C_4 alcohol blend (*1*), economic evaluation showed that this process was more convenient than the use of a conventional production process, with an olefine feedstock. Industrial research has devoted its efforts to the optimization of the process conditions (heat removal from the reactor, water removal, and alcohol phase purification) and to the development of new catalysts (*3–6*).

Catalysts based on high-pressure methanol catalysts (zinc–chromium oxides with alkaline promoters), on low-pressure methanol catalysts (Cu–Zn–Al(Cr) oxides with alkaline promoters), and on modified Fischer–Tropsch catalysts have been studied (*7–12*). In several cases, high-pressure conditions (100–200 atm, 350–400°C) were employed to obtain 20–30% of C_2^+OH in the alcohol blend. Nevertheless, thermodynamic calculations show that both the yield and the selectivity to higher alcohols are

0021-9517/89 $3.00

favored by the operative conditions of the low-pressure process, i.e., 60–100 atm and 250–320°C (*13*). Recently, the development of a new catalyst based on molybdenum sulfides which would produce more than 50% of C_2^+OH has been reported (*14*). Mixed oxide catalysts like Cu–Zn–Al(Cr) or Cu–Co–Al(Cr) modified by K, Th, Cs, or Mn have been proposed to operate under low-pressure conditions (*5, 15, 16*). The synthesis of these catalytic systems is normally achieved by using two main preparation steps. In the first step, a ternary precursor is obtained by coprecipitation and decomposed through thermal treatment. In the second step, the promoter is introduced by impregnation. The initial precursor homogeneity is an essential quality that should not be modified during the transformation steps of the solid. The coprecipitation method leads to ternary precursors which have often a rigidly defined stoichiometry and are seldom homogeneous due to the composition changes in the mother liquor.

In previous papers (*17, 18*) we have studied the precipitation conditions of the ternary Cu–Co–Al system (pH, temperature, neutralization method) to obtain a homogeneous hydrated precursor. Crystallized and amorphous precipitates of different R = (Cu + Co)/Al atomic ratios were prepared. In both cases, the ternary hydrotalcite phase $(Cu,Co)_6Al_2CO_3(OH)_{16} \cdot 4\ H_2O$ selectively appeared only in a narrow range of the atomic ratio R, thereby indicating that a rather rigid stoichiometry was necessary to obtain homogeneous precursors. This conclusion was in line with similar studies performed for Cu–Zn–Al precursors (*19, 20*).

The complexation method (*21–24*) was developed to obtain homogeneous precursors. Amorphous perfectly homogeneous mixtures are obtained by evaporating a solution containing all the metallic ions and a complexing polyfunctional hydroxyacid. In the case of quaternary catalysts, this method has the additional advantage that the alkaline promoter can be included from the start. However, the decomposition in air of these glassy precursors is often very rapid and exothermic. A high tendency to uncontrolled decomposition has been reported when the precursor contains a metal catalytically active in oxidation reactions (*25*). In these cases, the method cannot be easily used on an industrial scale.

In this paper we have studied the decomposition of Cu–Co–Al precursors obtained by the complexation method using citric acid as the polyfunctional hydroxyacid. Ternary precursors with different metallic composition were prepared, and the thermal decomposition on air and nitrogen streams was characterized by using differential thermal analysis, thermogravimetry, and IR spectroscopy. The advantage of performing a previous treatment in nitrogen at moderate temperatures in order to diminish the problems caused by the energetic decomposition in air is particularly discussed.

EXPERIMENTAL

The solid amorphous precursors were prepared according to the main steps reported in Ref. (*24*). In this technique, it is important to obtain the rapid dehydration of the solution at low temperatures. The citric acid was added to a concentrated aqueous solution which contained all the required ions as metal nitrates. In all the cases, an acid/metal ratio of 1 g-eq of acid/total g-eq of metals was used. The solution was first held at boiling temperatures for 20–30 min. After that, the solution was dehydrated under vacuum in a revolving flask at 75°C until viscosity was sufficiently high to interfere with discharging the vessel (approximately 500 cP at 20°C). Finally, dehydration was completed by drying in a vacuum oven at 80°C for 13 h. The precursors obtained after this procedure have the aspect of a solid foam uniformly colored. Flat diffractograms were obtained when the samples were characterized by X-ray diffraction. The metallic composition and the color of the precursors used in this work are presented in Table 1.

TABLE 1

Metallic Composition of the Cu–Co–Al Precursors Used in This Work

Precursor	Color	Theoretical atomic ratios		Metallic composition determined by AAS				
		$R = \frac{Cu + Co}{Al}$	$r = \frac{Cu}{Co}$	% Cu	% Co	% Al	R	r
A	Violet	1	1	6.0	5.9	5.6	0.9	0.9
B	Violet	3	1	10.3	8.8	2.7	3.1	1.1
C	Gray–violet	12	1	12.2	11.6	0.8	13.1	1.0
D	Deep violet	3	0.5	7.0	11.5	2.8	2.9	0.6
E	Light blue	3	5	16.5	3.2	2.9	2.9	4.8

The thermal decomposition of the precursors in air and nitrogen was studied by differential thermal analysis (DTA), thermogravimetry (TG), and derivative thermogravimetry (DTG) using a Shimadzu DT-30 thermal analyzer and a Cahn electrobalance. In DTA experiments, the temperature was raised 2°C min^{-1} within the temperature range of 20–600°C. Samples weighing 3–5 mg were heated in quartz dishes under the chosen atmospheres. When the thermal decomposition was studied through gravimetric techniques the temperature program corresponded to a nonuniform temperature rise. The rates were progressively varied from 1.2°C min^{-1} at 220°C to 5°C min^{-1} at 300°C and 7°C min^{-1} at 600°C. The amount of sample used was 10–15 mg. Nitrogen was carefully purified to remove water and traces of oxygen. In all the thermal measurements the flow rate of nitrogen and air was 40 ml min^{-1}.

IR spectra were obtained with Perkin–Elmer 330 equipment and were measured between 3900 and 600 cm^{-1}. Since we did not observe any relevant features between 3900 and 2000 cm^{-1}, the spectra in this paper are shown only between 2000 and 600 cm^{-1} for simplicity. The precursors as prepared were mixed with KBr and pressed into thin wafers.

The carbon content on the samples was measured by combustion volumetry. The metallic composition of the samples was determined by atomic absorption spectrometry.

RESULTS

1. Decomposition in Air: DTA and Thermogravimetric Results

The DTA curves corresponding to the decomposition in air of the precursors are presented in Fig. 1. In all the cases, a similar behavior characterized by the existence

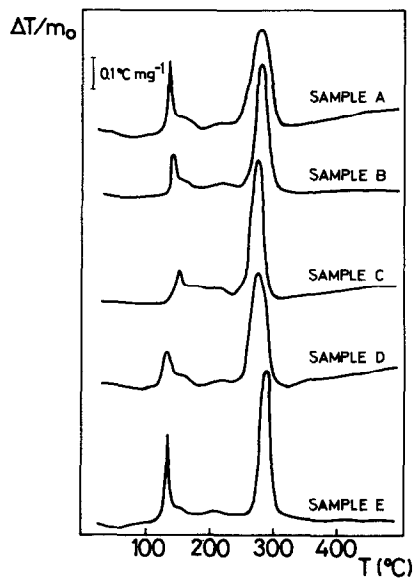

FIG. 1. DTA profiles of the decomposition of precursors in air. Heating rate, 2°C min^{-1}. The main characteristics of the samples are given in Table 1.

of two main exothermic transformations was verified. The low-temperature peak appeared at 135–145°C. By comparison of the samples with the same r ratio, it was observed that such a peak diminished when the R ratio increased (Fig. 1, samples A, B, and C). On the other hand, for a given R ratio the low-temperature peak increased when the relative Cu concentration was increased (Fig. 1, samples D and E of, respectively, $r = 0.5$ and $r = 5$). The high-temperature peak corresponded to a more important exothermic transformation and appeared in the region 275–285°C.

Two additional small bands which corresponded to exothermic transformations were also detected. A band appeared as a shoulder of the low-temperature peak, at 165–175°C. The other band was observed at approximately 220–230°C.

The decomposition of the precursors in air was also characterized by thermogravimetry. The DTG curves are given in Fig. 2. Qualitatively, the curves were similar to those obtained by DTA. However, the temperatures corresponding to the maxima of the peaks in Fig. 2 were approximately 15°C higher than those of Fig. 1. This shift must be attributed to the differences in the experimental devices and also the different rate in the temperature programming. Thus, the low-temperature peak appeared at 150–160°C. Regarding the high-temperature peak, it was verified that such a peak shifted to the lower temperatures when the R ratio was increased (Fig. 2, samples A, B, and C).

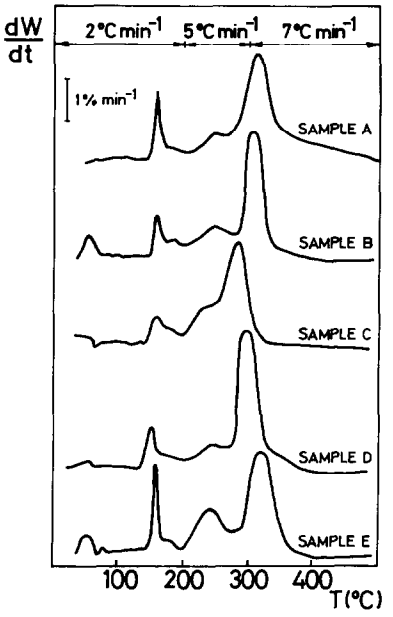

FIG. 2. DTG curves of the decomposition of precursors in air. In the ordinates, W represents the percentage weight loss.

As in the case of Fig. 1, two additional bands are observed: (i) a superimposed band which appeared as a small shoulder at the end of the low-temperature peak, and (ii) a second band at 240–250°C.

Quantitative results of the mass losses detected during the decomposition of the precursors in air are given in Table 2. The

TABLE 2

Weight Losses at Consecutive Temperature Ranges (in % of the Initial Weight)

Precursor	20–100°C		100–200°C		200–280°C		280–350°C		350–500°C		100–500°C	
	Air	N_2	Air	N_2	Air	N_2	Air	N_2	Air	N_2	Air	N_2
A	3.9	3.4	30.9	31.4	8.9	9.0	28.0	5.0	2.2	21.2	70.0	66.6
B	7.8	7.4	26.7	27.4	11.1	9.4	23.9	5.8	0.2	16.8	61.9	59.4
C	5.4	6.2	24.4	23.3	21.2	12.6	14.3	7.9	0.5	16.1	60.4	59.9
D	4.6	3.8	27.0	27.7	9.4	8.8	25.8	5.2	0.5	20.9	62.7	62.6
E	7.7	12.3	35.1	31.4	13.9	11.8	19.7	5.5	0.9	10.3	69.6	59.0

temperature ranges were chosen according to the general pattern of the curves of Fig. 2. Up to 100°C the mass loss corresponded mainly to the water removal from the precursors. The low-temperature peak (100–200°C range) represented approximately 25–35% of the initial weight. Considering samples A, B, and C which have the same Cu/Co ratio, the mass loss decreased from 30.9% (sample A, $R = 1$) to 24.4% (sample C, $R = 12$). In the region 200–280°C (which is the region corresponding to the intermediate band of Fig. 2) the weight loss of the samples was 9–14% except for sample C (21.2%). In this case, a part of the mass loss corresponded to the high-temperature peak since such a peak appeared at lower temperatures (Fig. 2). On the other hand, it seems that the weight loss increased when both the r and the R ratios were increased. The mass loss in the high-temperature peak range (280–350°C) represented approximately 20–30% of the initial weight of the samples except for sample C (14.3%). The lower weight loss registered for sample C is also explained by the shift of the high-temperature peak to the lower temperatures. As mentioned above, such a shift caused that part of the high-temperature peak to appear in the 200–280°C range. By comparison with the 200–280°C range, an opposite tendency was observed. In fact, the mass loss in the region 280–350°C diminished when the R (samples A and B) or r (samples D, B, and E) ratios were increased. In all the cases, no significant changes were observed above 350°C. If the weight corresponding to the water elimination was not considered, the total mass loss for the five samples was between 60 and 70% (Table 2, range 100–500°C).

In summary, the results given in Table 2 and Figs. 1 and 2 showed the following: (i) The decomposition of the precursors in air occurred through two important exothermic transformations. The weight losses corresponding to both transformations were of approximately 20–30%. (ii) An intermediate decomposition was also detected. It represented about 9–14% of the total weight and was slightly exothermic. (iii) The main characteristics of such transformations (heat evolution, quantity of lost mass, peak temperature) depended on the metallic composition of the samples, represented by the ratios R and r.

2. *Decomposition in N_2: DTA and Thermogravimetric Results*

The DTA curves obtained when the decomposition of the precursors was performed in N_2 are shown in Fig. 3. In all the cases, an exothermic peak with a shoulder at the end appeared at 138–150°C, and a small band was detected at approximately 220°C. The characteristics of these peaks were very similar to those obtained for the decomposition in air (Fig. 1, low-temperature peaks). No significant thermal effects were noted at higher temperatures; only sample C gave rise to an additional small band at 340°C.

The general pattern of DTG curves (Fig. 4) allowed us to distinguish between two main regions. In the region 20–280°C the DTG curves were very similar to those observed for the decomposition in air. On the contrary, above 280°C the decomposition in N_2 was clearly different from that performed in air. In fact, the high-temperature peak did not appear and a broad band with a

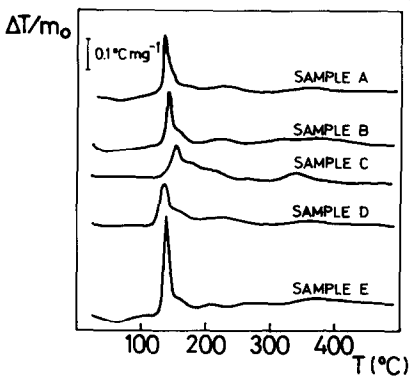

FIG. 3. DTA profiles of the decomposition of precursors in nitrogen. Heating rate, 2°C min^{-1}.

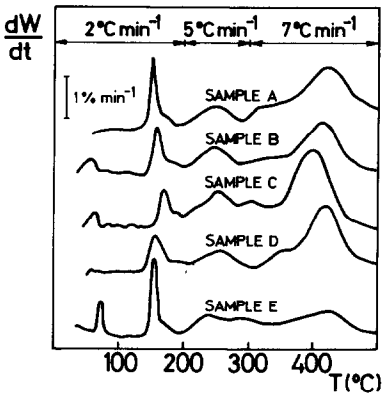

FIG. 4. DTG curves of the decomposition of precursors in nitrogen.

maximum at 400–420°C was detected in the region 350–500°C.

The TG results summarized in Table 2 confirmed that in the region of 20–280°C the decomposition of the precursors in air and N_2 occurred with similar weight loss. In the region 350–500°C the mass losses of the five precursors were 10–20% of the initial weight. It was observed that such a weight change diminished when the *r* ratio was increased (Table 2, samples D, B, and E). From the Table 2, range 100–500°C, it can also be observed that the total weights eliminated during the decomposition of precursors in N_2 were slightly lower than those corresponding to the decomposition in air.

3. Decomposition in Air and N_2: IR Spectroscopy Results

To obtain more insight into the decomposition phenomenon, additional experiments using IR spectroscopy were performed. The IR spectrum of the citric acid in the region 2000–600 cm^{-1} is presented in Fig. 5 (spectrum a). Literature data (*26–33*) provide a reliable identification of the principal absorption bands. In the region of the C=O stretching vibration a double carbonyl frequency was obtained. The peak at 1750 cm^{-1} is indicative of free carbonyl groups whereas the peak at 1700 cm^{-1} represents the carbonyl frequency of the coordinated carboxylic groups, i.e., groups showing internal hydrogen bonds. The bands in the ranges 1350–1430 and 1170–1250 cm^{-1} correspond respectively to the C–O stretching vibrations and to OH in-plane deformation vibrations. The OH stretching vibrations of the carboxyl group occur as a broad band with two superimposed peaks (OH bonded at 3500 cm^{-1} and intramolecular H-bond at 3300 cm^{-1}) in the region 3000–3600 cm^{-1}, and as a satellite band at 2600 cm^{-1}. Finally, the C–O stretching in the C–OH group and the tertiary OH are represented by the bands at 1080 and 1140 cm^{-1}, respectively.

The IR spectrum of precursor B is shown in Fig. 5 (spectrum b). Similar spectra were obtained for the other precursors; only minor changes in the relative intensity of the peaks were detected. In the solid citrate the carboxyl groups are ionized. The resonance between the two C–O bonds of the COO^- group results in the appearance of two new bands near 1600 and 1400 cm^{-1} which correspond to the antisymmetric and symmetric vibrations of the COO^- grouping (*29*). Since many other skeletal vibrations occur in the range 1400–1300 cm^{-1}, the band at 1600 cm^{-1} will be more characteristic to

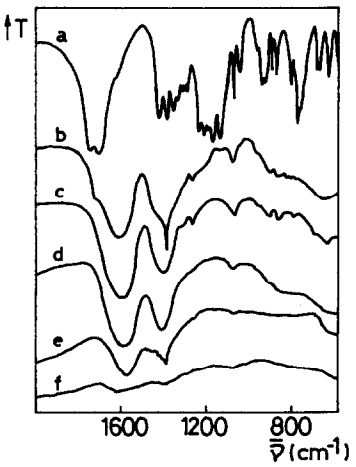

FIG. 5. IR study of the decomposition of precursors in N_2. Spectrum (a), citric acid. Spectrum (b), precursor B. Spectra (c, d, e, and f), precursor B decomposed in N_2 at respectively 200, 300, 400, and 500°C.

evaluate the carboxylate groups attached to metallic ions. The broad band at 3300–3500 cm^{-1} arises mainly from the presence of water. The other three small bands of spectrum b can be identified according to the IR characterization of the citric acid mentioned above. The C–O stretching in the C–OH group and the OH bending vibration appear at 1080 and 1250 cm^{-1}, respectively. The C=O stretching vibration which represents the acid groups not bonded to metal ions appears as a superimposed band at approximately 1700 cm^{-1}. Finally, the absorption band of the nitrate ions occurs as a sharp superimposed band at 1375 cm^{-1} (*34*).

The IR spectrum of precursor B after thermal decomposition in N_2 at 200°C is shown in Fig. 5 (spectrum c). Such a treatment caused the disappearance of the absorption bands corresponding to the nitrate ions (1375 cm^{-1}) and to the carbonyl absorption (the shoulder at 1700 cm^{-1} in the broad band between 1500 and 1800 cm^{-1} of spectrum b). No significant changes were observed when the decomposition temperature was increased to 300°C (spectrum d). The treatment with N_2 at 400°C caused the partial decomposition of the citric acid structure as is revealed by the intensity diminution of the carboxylate absorption bands (spectrum e). After decomposition at 500°C the citric acid structure was completely broken down (spectrum f).

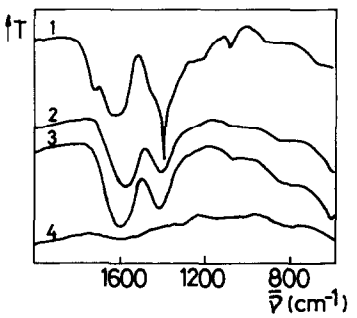

FIG. 6. IR spectra of the decomposition of precursor E. Precursor E (spectrum 1). Precursor E decomposed in N_2 at 220°C (spectrum 2), in air at 220°C (spectrum 3), and in air at 300°C (spectrum 4).

TABLE 3

Treatment in Air of Precursors Previously Decomposed in N_2 up to 500°C

Sample	% C[a]	Mass loss[b] (%)	Peak temp.[c] (°C)	ΔT[d] (°C)
A	11.9	19.7	350	70
B	8.2	14.7	350	70
C	<0.4	0	Not detected	—
D	8.3	15.4	330	52
E	8.7	15.4	325	35

[a] Carbon level before the air treatment.
[b] Mass loss in the range 100–500°C.
[c] Values determined in DTA experiments.
[d] ΔT is the difference between the peak temperature of this table (column 4) and those corresponding to the high-temperature peaks of Fig. 1.

Regarding the decomposition in air, Fig. 6 presents the IR spectra obtained for sample E. The precursor (spectrum 1) was decomposed at 220°C in air (spectrum 3) and N_2 (spectrum 2). Spectra 2 and 3 were very similar, thereby indicating that the precursor decomposition up to 220°C was not dependent on the atmosphere. As in the case of sample B (Fig. 5, spectrum c) the treatment at 220°C eliminated the absorption peaks corresponding to ionic nitrates (sharp peak at 1375 cm^{-1}) and to the carboxyl groups not bonded to metal ions (peak at 1700 cm^{-1}). When the decomposition in air was performed at 300°C, the citrate chains were completely oxidized (spectrum 4).

4. *Consecutive Decomposition in N_2 and Air*

The samples decomposed in N_2 at 500°C were submitted to an additional treatment in air from room temperature up to 500°C. The TG and DTA results are summarized in Table 3. The carbon levels determined after decomposition in N_2 and prior to the air treatment are also shown in Table 3.

Except for sample C, after the N_2 treatment a significant quantity of carbon remained on the decomposed samples. Such a carbon concentration diminished when the R ratio was increased (Table 3, samples

A, B, and C). By comparison, the carbon level was also determined in the same precursors directly decomposed in air to 500°C. In all the cases, the carbon concentration was lower than 0.5%.

The air treatment performed after the N_2 decomposition of the samples caused an exothermic transformation between 300 and 380°C which must be attributed to the carbon burning. Thus, when the C level was very low (sample C) the exothermic peak was not detected. The temperature maxima of the carbon burning peaks were compared to those of the high-temperature peaks of Fig. 1. According to IR spectra of Fig. 6, these high-temperature peaks arose mainly from the oxidation of the citric acid structure when the samples were directly decomposed in air (pyrolysis step). As is shown in Table 3, the temperatures of the carbon burning were 35–70°C higher than those of the corresponding high-temperature peaks in the pyrolysis step.

DISCUSSION

Chemical and infrared analysis indicated that the amorphous solid precursors are essentially mixed hydroxycitrates of the metals ions introduced. The polyfunctionality of the citric acid and the formation of chelate bonds favor two- and three-dimensional condensations which lead to a polymeric skeleton structure. Since these different bonds are randomly distributed, any kind of cation ordering in the three-dimensional networks must be discarded. This explains why the citrate precursors have an amorphous glass-like structure with no evidence of inhomogeneity. The citric acid chains in the precursor structure contain free carboxyl groups, carboxylate groups attached to metal ions, and intramolecular hydrogen bonds.

TG, DTA, and DTG results summarized respectively in Table 2 and Figs. 1 and 2 showed that the decomposition of the precursors in air occurred through the following transformations: (i) an exothermic low-temperature decomposition at 135–150°C, which represented 25–35% of mass loss; (ii) an intermediate transformation at 220–240°C and ΔW = 10–15%; and (iii) a highly exothermic decomposition at 280–300°C and ΔW = 20–25%. We will first analyze the low-temperature decomposition. IR spectra of Fig. 6 showed that calcining at 200°C eliminated most of the ionic nitrates and free carboxyl groups. Hydrated metal nitrates do not decompose in simple stages but in a number of separate and endothermic processes (*35, 36*). The main decomposition step of the citric acid molecule is dehydration at 180–200°C to give aconitic acid through an endothermic transformation (*37*). On the other hand, the DTA, DTG, and IR spectroscopy results showed that in the low-temperature region (i.e., $T <$ 280°C) the decomposition mechanism was not dependent on the atmosphere since similar results in N_2 and air were obtained. Thus, the exothermic low-temperature peak cannot be explained either by a separate degradation process of the citrate chains like decarboxylation or dehydration or by a chemical oxidation caused by the O_2-containing atmosphere used in the decomposition. The most probable explanation is that an internal exothermic reaction between nitrates and free carboxyl groups like

$$NO_3^- + 3\,(COOH) \rightarrow NO + H_2O + 3\,CO_2 + OH^-$$

takes place. A similar reaction was proposed by Courty *et al.* (*24*) to explain the production of CO_2 which occurs during the vacuum evaporation of the solution in the first step of the preparation of precursors. Thus, the fact that the low-temperature peak was more important in the case of the decomposition of precursors A (high Al content) and E (high Cu/Co ratio) suggests that these precursors had a higher content of uncombined citric acid. Such an explanation is supported by the IR spectra of precursors which showed that the superimposed band at 1700–1750 cm^{-1} assigned to free acid groups was clearly more defined in

the case of samples A and E. It has already been noted that the amount of the nitrate ions in the precursors varies in a complementary way to the combined citric acid (*31*). Thus, it seems that the presence of nitrate ions is connected with the fact that the reaction between citric acid and metal nitrates was not allowed to go to completion (*33*).

The intermediate decomposition at 220–240°C was not dependent on the atmosphere and occurred without significant thermal evolution. Also, the IR characterization did not reveal any important change either in the peak intensity or in the vibration frequencies, thereby indicating that the citrate chains were essentially preserved. The intermediate transformation would probably represent an internal dehydration in the vitreous matrix (*38, 39*).

The high-temperature decomposition corresponded to the energetic oxidation of the citrate chains. In all the cases, the carbon level remaining on the samples after such a pyrolysis step was lower than 0.5%. The oxidation peak was shifted to the lower temperatures when the R ratio was increased showing the catalytic effect of (Cu + Co) loading on the oxidation reaction. The fact that the presence in the precursors of metals whose oxides are oxidation catalysts (i.e., Ag, Cu, Co, Ni, Fe) accelerates the pyrolysis step has already been noted (*25, 31*). In our case, the catalytic effect of Cu and Co on the burning by atmospheric oxygen of the citrate chains caused a high tendency to uncontrolled decomposition. In fact, only when experiments were performed using low sample weight or when samples were carefully arranged in consecutive thin layers separated by inert material, were the overall decomposition patterns of Figs. 1 and 2 which showed two main exothermic transformations obtained. For higher sample weight, the energetic decomposition caused the extensive reaction of precursors with rapid evolution of the product gases which led to the fluidization of the bed with particle projection. It seems that the increase in the particle temperature caused by the exothermia of the low-temperature decomposition was sufficient to promote the oxidation reactions of the second decomposition step. Thus, the overall decomposition of precursors occurred through a highly exothermic one-step decomposition which is difficult to control. One possibility to avoid this uncontrolled decomposition is to support the citrate complex on a porous carrier (*40*). Another possibility would be to reduce the oxygen concentration in the nitrogen–oxygen mixtures.

As a limiting case, we have studied the decomposition of precursors in a nitrogen atmosphere (Table 2 and Fig. 3, 4, and 5). As was mentioned above, the thermal decompositions in N_2 and air up to 280°C were similar. Above 280°C, the DTG and DTA patterns in N_2 were clearly different from those obtained in air. In fact, in N_2 the breakup of citrate chains occurred in several consecutive transformations without measurable thermal effect. After the N_2 treatment up to 500°C the IR bands at 1600 and 1400 cm^{-1} assigned to COO^- grouping completely disappeared. However, except for sample C, a significant quantity of carbon remained on the sample (Table 3). This result is in line with the work of Galwey (*41*), who found that the thermal decomposition under vacuum of similar vitreous metal complexes yielded an intimate mixture of carbonaceous polymers and metal oxides. The carbon level of decomposed samples increased when the relative Al concentration of the precursors was increased. This result could be explained by considering that the formation of alumina in the vitreous matrix decreases the mobility and diffusion of the ligands and radicals which take part in the reaction leading to the product gases. A similar high-temperature decomposition mechanism which implies rupture of covalent bonds in the homogeneous reactant matrix has been proposed to account for the thermal decomposition *in vacuo* of synthetic aluminium

mellitate (*38*). In such a decomposition model, the reaction will occur by a bimolecular process involving two citrate radicals of limited freedom of movement in the glass-like structure by interchange of bonds between the different ligands. As the alumina content in the vitreous phase increases, the mobility of the ligands decreases. When sufficient alumina is present the formation of the decomposition transition complex is preserved and the reaction ceases.

It is significant to note that in the case of precursor C the decomposition in N_2 up to 500°C eliminated almost completely the organic carbon and so an additional treatment in air to oxidize the residual carbon will not be necessary. Since the oxidation state of the metal components of resulting mixed oxides depends on the decomposition atmosphere, the possibility of using only an inert atmosphere could be important. In the ternary Cu–Co–Al system, it must be expected that the kind of atmosphere used in the decomposition step will determine mainly the oxidation state of Co ions. In our case, the metallic composition of industrial catalysts is defined in the range $R \leq 3$ and $r \geq 1$ (*15*). For such a composition range the carbon content remaining on the samples after the decomposition in N_2 was approximately 8–10%.

To eliminate the carbonaceous polymers, the samples were treated in air (Table 3). The coke burning took place at 300–350°C. Such a temperature was 40–70°C higher than the temperature corresponding to the oxidation of citrate chains when the precursors were directly decomposed in air. The most probable reasons to explain such a shift of the carbon oxidation peak are the following: (i) the carbon remaining on the samples after the N_2 treatment at 500°C is less hydrogenated, and (ii) the semidecomposed precursors in air or N_2 up to 280°C have widely open pores which favor the reaction of the citrate chains with oxygen in the pyrolysis step (*31*). If the decomposition of precursors is performed up to 500°C the formation of metal oxides leads to more crystallized structures which will make the diffusion of the oxygen molecules difficult and as a result the oxidation peak temperature increases.

In conclusion, the use of an inert atmosphere in the thermal decomposition of the precursors diminishes the possibility of an uncontrolled decomposition since the pyrolysis step does not take place. Nevertheless, after the breakup of the citrate chains a significant quantity of carbon remains on the sample making necessary an additional treatment in air at high temperatures to eliminate it. It seems that a two-step decomposition procedure using first nitrogen up to 280°C and after that an oxygen-containing atmosphere to oxidize the organic part at relatively low temperature will be more appropriate to avoid the danger of an uncontrolled exothermic decomposition (direct decomposition in air) or the problems derived from a contamination with residual carbon (decomposition in N_2 up to 500°C). In a second part we will analyze the influence of these different decomposition treatments on the resulting mixed oxides, especially regarding homogeneity and local interactions between Cu and Co which are the active centers of this kind of catalyst.

ACKNOWLEDGMENTS

Support of this work by the Consejo Nacional de Investigaciones Científicas y Técnicas (CONICET) and the Secretaría de Estado de Ciencia y Tecnología (Argentina) is gratefully acknowledged.

REFERENCES

1. Laux, P. G., "Proceedings, Int. Symp. Alcohol Fuel Technology," Pap. 3–5, 1977.
2. Greene, M. I., *Chem. Eng. Prog.* **78**(8), 46 (1982).
3. Paggini, A., Lagana, V., Manara, G., and Fattore, V., Fr. Demande Br. 2,490,215, Snamprogetti SPA, 1981.
4. Sugier, A., and Freund, E., U.S. Patent 4,112,110, Institut Francais du Pétrole, 1978.
5. Hardman, H., and Beach, R., U.S. Patent Appl. 905,703, Standard Oil Co., 1978.

6. Greene, M., and Gelbein, A., U.S. Patent 4,477,594, Chem. Systems Inc., 1984.
7. Leonov, V. E., and Kalinichenko, L. M., *Khim. Tverd. Topl.* **15**(1), 26 (1981).
8. Smith, K. J., and Anderson, R. B., *Canad. J. Chem. Eng.* **61,** 40 (1983).
9. Vedage, G. A., Himelfarb, P., Simmons, G. W., and Klier, K., "Solid State Chemistry in Catalysis" (R. K. Grasselli and J. F. Brazdil, Eds.), Chap. 18, p. 295. American Chemical Society, Washington, DC, 1985.
10. Hindermann, J. P., Razzaghi, A., Breault, R., Kieffer, R., and Kiennemann, A., *React. Kinet. Catal. Lett.* **26,** 221 (1984).
11. Arakawa, H., Fukushima, T., Ichikawa, M., Natsushita, J., Takeuchi, K., Matsuzaki, T., and Sugi, Y., *Chem. Lett.*, 881 (1985).
12. Chen, Yu-Wen, *Canad. J. Chem. Eng.* **64,** 875 (1986).
13. Marchi, A. J., and Apesteguía, C. R., *React. Kinet. Catal. Lett.* **31**(1), 107 (1986).
14. Haggin, J., *Chem. Eng. News,* 29 (1984).
15. Courty, Ph., Durand, D., Freund, E., and Sugier, A., *J. Mol. Catal.* **17,** 241 (1982).
16. Hofstadt, C. E., Schneider, M., Bock, O., and Kochloefl, K., "Proceedings, 3rd Int. Symp. on Scientific Bases for the Preparation of Heterogeneous Catalysts," pp. 709, 721. Elsevier, Amsterdam, 1983.
17. Marchi, A. J., Sedran, A. G., and Apesteguía, C. R., "Proceedings, 4th Int. Symp. on Scientific Bases for the Preparation of Heterogeneous Catalysts, Louvain-la-Neuve, Belgium," Pap. H-7, 1986.
18. Marchi, A. J., Di Cosimo, J. I., and Apesteguía, C. R., "Proceedings, 9th International Congress on Catalysis," (M. J. Phillips and M. Ternan, Eds.), pp. 529–536. The Chemical Institute of Canada, Ottawa, 1988.
19. Gherardi, P., Ruggeri, O., Trifiro, F., and Vaccari, A., "Proceedings, 3rd Int. Symp. on Scientific Bases for the Preparation of Catalysts," pp. 723–731. Elsevier, Amsterdam, 1982.
20. Busetto, C., Del Piero, G., Manara, G., Trifiro, F., and Vaccari, A., *J. Catal.* **85,** 260 (1984).
21. Paris, J., and Paris, R., *Bull. Soc. Chim. Fr.* **4,** 1138 (1965).
22. Rousset, A., and Paris, J., *Bull. Soc. Chim. Fr.*, 446 (1969).
23. Marcilly, Ch., Courty, Ph., and Delmon, B., *J. Amer. Ceram. Soc.* **53,** 56 (1970).
24. Courty, Ph., Ajot, H., and Marcilly. Ch., *Powder Technol.* **7,** 21 (1973).
25. Shannon, I. R., *Chem. Ind.*, 149 (1971).
26. Colthup, D. H., *J. Opt. Soc. Amer.* **40,** 397 (1950).
27. Kirschner, S., *J. Amer. Soc.* **78,** 2372 (1956).
28. Goulden, J. D. S., *Spectrochim. Acta* **16,** 715 (1960).
29. Larsson, R., *Acta Chem. Scand.* **19,** 783 (1965).
30. Bellamy, L. J., "The Infrared Spectra of Complex Molecules." Methuen, London, 1958.
31. Delmon, B., and Droguest, J., "Fine Particles," Second Int. Congr. (E. W. Kuhn and J. Ehretsmann, Eds.), p. 242. Princeton Univ. Press, Princeton, NJ, 1974.
32. Pouchert, C. J., "The Aldrich Library of Infrared Spectra," 3rd ed. Aldrich Chem. Co., Milwaukee, 1981.
33. Zhang, H. M., Teraoka, Y., and Yamazoe, N., *Chem. Lett.* **4,** 665 (1987).
34. Miller, F. A., and Wilkins, C. H., *Anal. Chem.* **24,** 1253 (1952).
35. Pierron, E. D., Rashkin, J. A., and Roth, J. F., *J. Catal.* **9,** 38 (1967).
36. Taylor, T. J., Dollimore, D., and Gamlen, G. A., *Thermochim. Acta* **103,** 333 (1986).
37. Barbooti, M. M., and Al-Sammerrai, D. A., *Thermochim. Acta* **98,** 119 (1986).
38. Galwey, A. K., *J. Chem. Soc.*, 5433 (1965).
39. Maslowska, J., Bielawsky, M., and Baranowska, A., *Thermochim. Acta* **92,** 235 (1985).
40. Courty, Ph., Raynal, B., Rebours, B., Prigent, M., and Sugier, A., *Ind. Eng. Chem. Prod. Res. Dev.* **19,** 226 (1980).
41. Galwey, A. K., *J. Chem. Soc. Sect. A,* 87 (1966).